Journal of Human Genetics (2019) 64:711–719
https://doi.org/10.1038/s10038-019-0609-1

ARTICLE

# Clinical and genetic analysis of patients with primary ciliary dyskinesia caused by novel *DNAAF3* mutations

Zhuoyao Guo[1] · Weicheng Chen[2] · Jianfeng Huang[1] · Libo Wang[1] · Liling Qian[1]

Received: 8 February 2019 / Revised: 30 March 2019 / Accepted: 31 March 2019 / Published online: 12 June 2019


## Abstract

Primary ciliary dyskinesia (PCD) is a rare phenotypically and genetically heterogeneous disorder resulting from abnormal cilia ultrastructure and function. Few studies have reported the phenotype and genetic characteristics of PCD caused by mutations in *DNAAF3*. In this study, four PCD patients with *DNAAF3* mutations underwent extensive clinical assessments, cilia ultrastructural and motion evaluations. All patients presented with situs inversus totalis, neonatal respiratory distress, and sinusitis; however, they did not have recurrent infections of the lower airways. The nasal nitric oxide level of these patients was markedly reduced. The respiratory cilia were found to be uniformly immotile, with their dynein arms defects. A total of 7 (5 novel) variants in *DNAAF3* were identified and cosegregated in their families by Trio-based whole-exome sequencing. As the first report on *DNAAF3* mutations in PCD patients in China, our study not only contributes to a deeper appreciation of the phenotypic characteristics of patients with *DNAAF3* mutations but also expands the spectrum of *DNAAF3* mutations and may contribute to the genetic diagnosis of and counseling for PCD.

## Introduction

Primary ciliary dyskinesia (PCD) is an infrequent autosomal-recessive or X-linked disease with an estimated prevalence of 1/20,000 [1]. Due to the impaired motile ciliary function, subsequent respiratory infections, situs inversus, and infertility are hallmarks of PCD [2]. The normal structure of the "9+2" axoneme of motile respiratory cilia in a transverse section includes nine peripheral outer doublets surrounding a central microtubule pair. Each doublet with inner dynein arms (IDA) and outer dynein arms (ODA) is associated with nexin links and is connected by radial spokes to the central pair [3]. Owing to a host of proteins that are involved in ciliary motility and ciliogenesis, PCD is a highly genetically heterogeneous disorder. To date, a total of 42 known PCD-causing genes have been identified, all of which encode proteins involved in ciliary structure, function, and ciliogenesis [1, 4–6]. Similarly, phenotypic heterogeneity of PCD is also extensive. The course of disease, nNO level, ciliary ultrastructure, and function vary greatly in different PCD patients, which significantly increases the complexity of the prognostic evaluation and diagnosis. Gratifyingly, recent advances in PCD genetics have identified a strong correlation between the phenotype and genotype [7, 8].

As a gene when mutated causes PCD, dynein axonemal assembly factor 3 (*DNAAF3*) (OMIM: 614566, also known as *PF22*) was first reported in 2012 [9] and only 9 mutations have been reported in ClinVar database (the last accessed date: March 23, 2019) (Fig. 1). *DNAAF3* is a cilia-related gene that encodes a 608-amino acid cytoplasmic protein that is important for the preassembly and transport of dynein arms from cytoplasmic assembly site into the axoneme. Mutations of *DNAAF3* prevent the correct assembly and transport of ODA and IDA, impacting the motility of respiratory cilia and leading to PCD. However, until recently, only a few cases of PCD with mutations in

These authors contributed equally: Zhuoyao Guo, Weicheng Chen

**Supplementary information** The online version of this article (https://doi.org/10.1038/s10038-019-0609-1) contains supplementary material, which is available to authorized users.

✉ Libo Wang
wanglbc@163.com

✉ Liling Qian
llqian@126.com

1 Respirology Department, Children's Hospital of Fudan University, 399 Wan Yuan Road, Shanghai 201102, PR China

2 Cardiothoracic Surgery Department, Children's Hospital of Fudan University, 399 Wan Yuan Road, Shanghai 201102, PR China

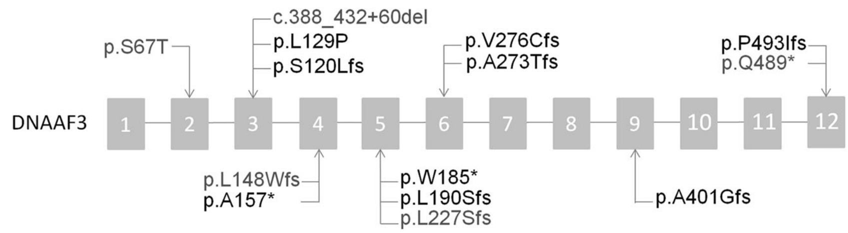


**Fig. 1** Schematic drawing of *DNAAF3*. The positions of all identified mutations are indicated, and novel mutations identified in the present study are indicated in red

*DNAAF3* have been reported, and its clinical characteristics and ciliary phenotype have not been studied thoroughly.

In this study, we systematically evaluated the phenotype and genetic characteristics of patients with *DNAAF3* mutations in four Chinese families. It is hoped that the detailed phenotype information identified in our study will help to better delineate the phenotypic characteristics of PCD patients and contributes to the growing number of candidate mutations in *DNAAF3*.

## Material and methods

### Patients and clinical materials

The study protocol was approved by the Ethics Committees of Children's Hospital of Fudan University, and written informed consent was obtained from all family members participating in this study. The clinical data of patients with *DNAAF3* mutations were retrospectively summarized. The diagnosis of PCD was based on the clinical findings, high-speed video microscopy analysis (HSVA), transmission electron microscopy (TEM), nasal nitric oxide (nNO) levels, and genetic testing, in accordance with the European Respiratory Society guidelines for the diagnosis of PCD [10].

### Measurement of nNO

Measurements of nNO were obtained from patients with the use of an EcoMedics CLD88 chemiluminescence NO analyzer (Dürnten, Switzerland); the aspiration sampling rate was 330 ml/min as recommended by the manufacturer. The measurement of nNO in cooperative children was performed according to the American Thoracic Society and European Respiratory Society guidelines [11]. For uncooperative children, nasal sampling was performed for 60 s during tidal breathing [12]. Measurements were recorded in parts per billion (ppb) and converted into a nNO production rate in nl/min with the following equation: nNO (nl/min) = NO (ppb) × sampling rate (ml/min).

### Transmission electron microscopy examination

To understand the abnormalities in the ultrastructure of the respiratory cilia, cilia were examined by means of electron microscopy at the Department of Electron Microscopy, Fudan University. Samples of nasal mucosa were fixed in 2.5% glutaraldehyde in 0.1 M sodium cacodylate buffer at 4 °C, washed overnight, and postfixed in 1% osmium tetroxide. After dehydration, the samples were embedded in epoxy resin. After polymerization, several sections were picked out onto copper grids. The sections were stained with aqueous 1% uranyl acetate and Reynold's lead citrate. Ciliary ultrastructural analysis was carried out using a transmission electron microscope (JEM-1400; Jeol, Tokyo, Japan).

### Immunofluorescence of the respiratory epithelium

Cells were treated with 4% paraformaldehyde, 0.2% Triton X-100, and 1% milk prior to incubation with primary (overnight at 4 °C after 1 h at 37 °C) and secondary antibodies (2 h at room temperature). Rabbit polyclonal anti-DNAH5 (1:1000) were obtained from Abcam (Taufkirchen, Germany). Mouse monoclonal anti-acetylated α-tubulin antibodies (1:1000) were obtained from Abcam. Highly cross-adsorbed secondary antibodies goat anti-mouse Alexa Fluor 488 (1:1000) and goat anti-rabbit Alexa Fluor 647 (1:1000) were from Abcam. DNA was stained with DAPI (1:1000) from Beyotime (Shanghai, China). Confocal images were taken on a Leica TCS SP8 confocal laser scanning microscope (Leica, Jena, Germany).

### High-speed video microscopy analysis

Nasal tissue was obtained from each patient and suspended in L-15 medium (Invitrogen, CA) for video microscopy using a Leica inverted microscope (Leica DMI300B) with a 67× oil objective under differential interference contrast optics. Movies were recorded at 200 frames/s at room temperature by use of a 680 PROSILICA GE camera (Allied Vision, PA), and digital recordings were evaluated by a blinded panel of co-investigators (Weicheng Chen, Zhuoyao Guo, Liling Qian). The ciliary beat frequency was obtained from an analysis of the video sequences. To assess other abnormalities in ciliary motion, we examined the ciliary beat pattern by using slow motion playback of the video sequence to generate tracings of the ciliary beat. In normal nasal epithelia, the ciliary beat pattern is characterized by metachronal waves composed of forward and reverse strokes synchronously sweeping in a planar motion across the respiratory epithelium (Supplementary Video 1).

### Whole exome sequencing (WES) and Sanger sequencing

Genomic DNA was extracted from the whole blood of the patients and their parents using the QIAamp DNA Blood Mini kit (Qiagen, Hilden, Germany). The DNA concentration was measured using a Nano-Drop spectrophotometer (Thermo Fisher Scientific, Waltham, MA). Trio-based WES was performed to search for potential genetic defects at the molecular genetic diagnosis center of Fudan University. Briefly, whole exomes were captured using an Agilent SureSelect Human All ExonV5 Kit (Agilent, CA, USA) and sequenced on an Illumina HiSeq 2000 platform. The average depth of the sequencing data was ≥90×. More than 95% of the targeted regions were sequenced with a coverage ≥20×, and low-quality reads were discarded. Remaining sequencing reads were aligned to the human reference genome (UCSC hg19) with Burrows-Wheelchair Aligner (BWA version 0.7.9a). Picard version 1.115 was used to remove any duplicate paired-end reads. Base quality score recalibration, local realignment around indels, single-nucleotide variants (SNVs), and insertion/deletions (indels) were called by the Genome Analysis Tool Kit (GATK version v3.2) [13].

Variants were annotated by VEP and ANNONVAR with databases Human Gene Mutation Database (HGMD, professional version), Clinvar, and OMIM (Online Mendelian Inheritance in Man) [14]. Our own databases and public databases including the Exome Aggregation Consortium (ExAC), 1000 Genome Project, Genome Aggregation Database (gnomAD), and Single Nucleotide Polymorphism Database (dbSNP) were used to filtering out common variants (minor allele frequency >1%). Intronic variants, synonymous variants were also discarded [14]. The protein functional consequence of variants was assessed with SIFT, PolyPhen2, and MutationTaster. We classified the candidate variants with reference to the ACMG guideline [15] based on allelic frequency, characteristics of the pedigree (homozygous, compound heterozygous in patients, heterozygous in parents [16]), compatibility with phenotypes, function prediction, and relevant literature. Particular attention was paid to variants in PCD and potential ciliary genes.

Sanger sequencing using a 3500XL Genetic Analyzer was conducted to validate the candidate variants identified by WES, and segregation analyses were performed in family members. The primer pairs used to amplify fragments encompassing individual variants were designed by Primer 3 and the sequences of the PCR primers are provided in Supplementary Table 1.

The RefSeq accession numbers of the transcript and corresponding protein isoform we used for mutation nomenclature were NM_001256714.1 and NP_001243643.1

### cDNA analysis

To determine the effect of these mutations on transcripts, RT-PCR was employed, using RNA from nasal epithelial cells. Total RNA was isolated from the nasal tissue of the patients by RNeasy Mini Kit (Qiagen, Germany). Subsequently, RNA was reverse-transcribed into cDNA using a first-strand cDNA synthesis kit (Takara, China). cDNA of the *DNAAF3* gene was amplified by polymerase chain reaction with specific primers. Then, 2% agarose gel electrophoresis and sequence analysis were performed. The primer sequences are provided in Supplementary Table 2.

## Results

### Clinical data

In the present study, we identified 4 Chinese patients (2 boys and 2 girls) from 4 unrelated families. The age of diagnosis of PCD ranged from 1 month to 10 years old. All individuals displayed unexplained neonatal respiratory distress and shortness of breath starting after a few hours of life and needed supplemental oxygen. Intriguingly, recurrent lower respiratory tract infection, which is a characteristic manifestation of PCD, was not present in these patients. The detailed clinical manifestations and latest medical examination of each patient are summarized in Table 1.

As an 11-year-old boy, P1 had a course of more than 10 years with an intermittent productive cough and runny nose. The boy had multiple episodes of mild upper respiratory infections during the preschool period but this condition spontaneously went into remission over the last 6 years. Chest CT scanning showed localized consolidation and atelectasis of the middle lobe of the left lung (Fig. 2a).

P2 was a 20-month-old boy from a consanguineous family. After the neonatal period, at 8 months of age, the boy was hospitalized due to repeated cough and wheezing. A few rhonchi were noticed by lung auscultation; chest CT scanning showed no significant lesions, while evident heart inversions were noticed (Fig. 2b). He was hospitalized for 5 days; received treatments, such as anti-infection therapy and anti-asthma by aerosol inhalation; and discharged after symptom improvement. His intermittent cough and nasal congestion remained for approximately 2 months and then spontaneously and markedly improved over the last 10 months.

P3 was a 16-month-old girl. She had presented to the respiratory department due to cough and nasal congestion for 2 days, at 10 months of age. Physical examination

**Table 1** Phenotypic features of individuals with identified *DNAAF3* mutations

| Characteristics | P1 | P2 | P3 | P4 |
|---|---|---|---|---|
| Known consanguinity | No | Yes | No | No |
| Gender | Male | Male | Female | Female |
| Age at PCD diagnosis | 1 month | 8 months | 10 months | 10 years |
| Age at last follow-up | 11 years | 20 months | 16 months | 18 years |
| High | 137 cm | 72 cm | 73 cm | 154 cm |
| Weight | 31.5 kg | 8.9 kg | 9.1 kg | 41.5 kg |
| Lung auscultation | Little rhonchi | No abnormality | No abnormality | Coarse moist rale in bilateral lungs |
| Birth status | Full-term natural labor with a weight of 2.3 kg | Full-term natural labor with a weight of 3.1 kg | Full-term natural labor with a weight of 3.0 kg | Full-term natural labor with a weight of 3.5 kg |
| Situs inversus | Yes | Yes | Yes | Yes |
| Neonatal respiratory distress | Yes | Yes | Yes | Yes |
| Respiratory symptom | Intermittent wet cough | Bronchitis, intermittent cough | Intermittent wet cough | Year-round dry cough |
| Respiratory microbiology | Negative | NA | NA | Negative |
| Otitis media | Unknown | Yes | Unknown | No |
| Hearing problems | No | Yes | No | No |
| Sinusitis | Yes | Yes | Yes | Yes |
| Smell problems | No | Unknown | Unknown | No |
| Respiratory function test | Mild obstructive ventilator dysfunction | NA | NA | Mild obstructive ventilator dysfunction |
| Nasal nitric oxide (nl/min) | 16.3 | 9.1 | 1.4 | NA |
| FeNO | NA | No abnormality | NA | No abnormality |
| FEV1, % pred | 98.7% | NA | NA | 96.5% |
| Chest CT | Localized consolidation; visceral inversion | Visceral inversion | Visceral inversion | Bronchiectasis; visceral inversion |
| CBF | 0 | 0 | 0 | 0 |
| TEM | DAs faintly recognizable | ODA + IDA defects | ODA + IDA defects | ODA + IDA defects |
| Comorbidities | NO | NO | NO | NO |

*FeNO* fractional exhaled nitric oxide, *FEV1* forced expiratory volume in 1 s, *FVC* forced vital capacity, *NA* not available, *IDA* inner dynein arm, *ODA* outer dynein arm, PFT pulmonary function test, *TEM* transmission electron microscopy

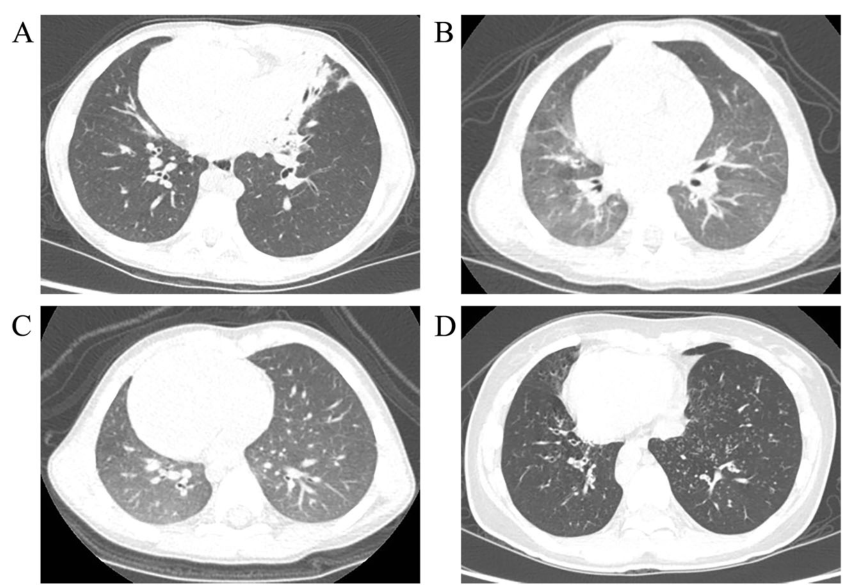


**Fig. 2** Chest CT images of the patients. **a** The chest CT scale of P1 showed consolidation and atelectasis of the middle lobe of the left lung; **b**, **c** CT images of P2 and P3 showing no abnormality except for dextrocardia; **d** chest CT of P4 showing centrilobular nodules distributed diffusely in the lower lung lobes with local bronchiectasis

showed no abnormality except for dextrocardia. No obvious abnormality was noticed in CT scans of the lung (Fig. 2c). The girl received symptomatic treatment. During a follow-up period of 6 months, the girl caught a cold but recovered quickly without treatment.

P4 had been receiving treatment in our hospital due to recurrent pneumonia over the last 2 years and is currently 12 years old. CT of her chest showed centrilobular nodules distributed diffusely in the lower lung lobes with localized bronchiectasis (data not shown). After discharge, the girl was asked to attend clinics annually. Aside from year-round dry cough, the girl's condition has been quite good without recurrent respiratory tract infections nor rhinorrhea. Her lung function and chest CT have been relatively stable compared with those from 6 years ago (Fig. 2d, Supplementary Table 3).

## Measurement of nNO

The nNO levels of P2 and P3 were measured during tidal breathing, while that of P1 was measured during oral exhalation against resistance. The nNO levels of these children are presented in Table 1 and are far below the recommended diagnostic cut-off (77 nl/min for oral exhalation against resistance, 47.4 nl/min for tidal breathing [17]).

## Ciliary structural and functional analysis

HSVA was performed and showed that the nasal cilia were immotile in all patients (Supplementary Video 2). At least 30 cilia cross-sections were examined by TEM and showed the loss of both ODA and IDA in P2, P3, and P4 (Fig. 3b–d) compared to normal cilium (Fig. 3e). However, the ciliary ultrastructure of P1 was equivocal (Fig. 3a). To further characterize the cilia ultrastructural defect, we performed high-resolution IF analyses, and confirmed that ODA were absent in the cilia of P1 (Fig. 4).

## Genetic characteristics and cDNA analysis

WES analysis of the genome demonstrated homozygous mutations of *DNAAF3* in P2 and compound heterozygous

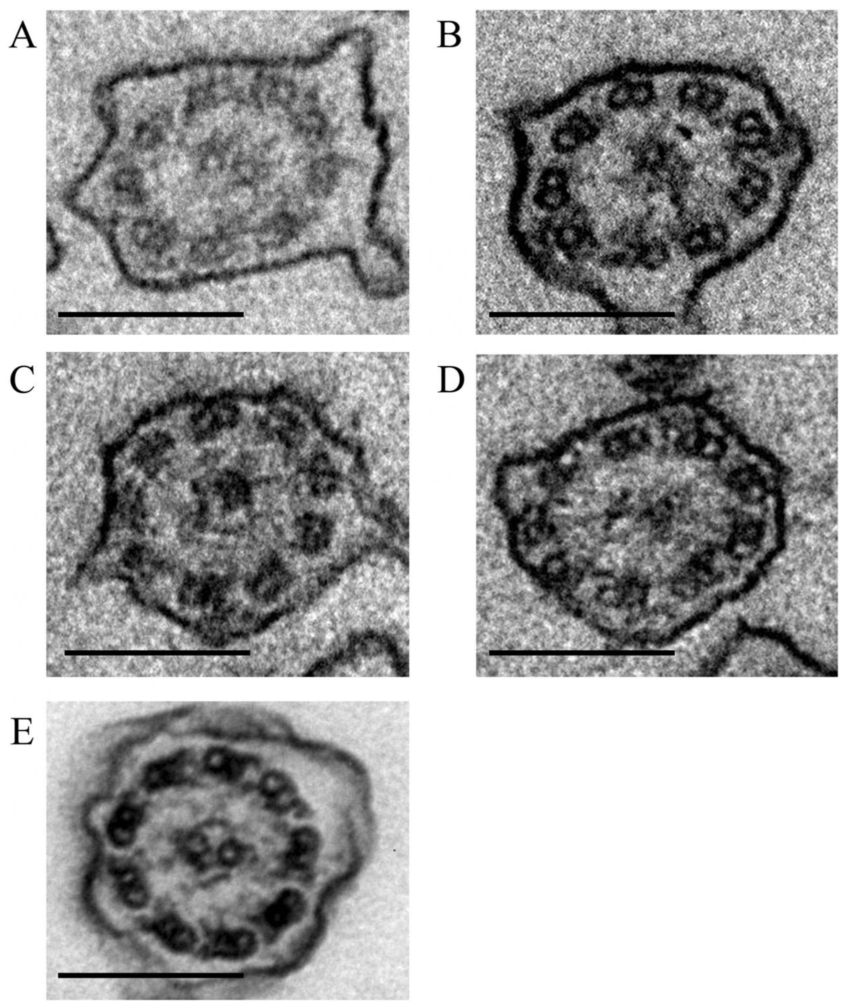


**Fig. 3** Structural analysis of the respiratory cilia. Representative cilia cross-sections are shown within the same micrograph (**a**); the ciliary ultrastructural of P1 was equivocal and missing the outer dynein arms (**b**–**d**). Scale bar, 0.2 μm

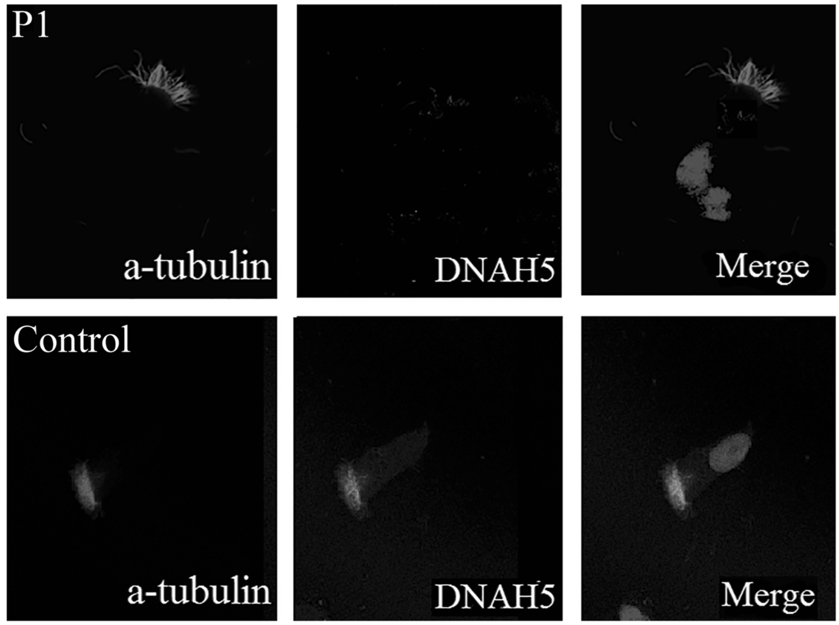


**Fig. 4** Anti-alpha-tubulin was used to label the cilia axoneme (red). DNAH5 (green) localizes along the entire cilia in cells from the unaffected control, but complete absence of DNAH5 protein from axonemes from P1

**Table 2** *DNAAF3* mutations of four patients from four families

| Patient | Mutations | Allele | Location | Type | Protein effect | HGMD |
|---|---|---|---|---|---|---|
| P1 | c.442delC | Pa | Exon4 | Frameshift | p.L148Wfs*13 | NA |
| | c.1465 C>T | Ma | Exon12 | Nonsense | p.Q489* | NA |
| P2 | c.679delC | Pa | Exon5 | Frameshift | p.L227Sfs*28 | NA |
| | c.679delC | Ma | Exon5 | Frameshift | p.L227Sfs*28 | NA |
| P3 | c.811_815dupGACGC | Pa | Exon6 | Frameshift | p.A273Tfs*13 | NA |
| | c.200 C>A | Ma | Exon2 | Missense | p.S67Y | NA |
| P4 | c.388_432+60del | Pa | Exon3 | Frameshift | N/A | NA |
| | c.811_815dupGACGC | Ma | Exon6 | Frameshift | p.A273Tfs*13 | NA |

*NA* not available

mutations in P1, P3, and P4 (Table 2). All of these mutations were confirmed by Sanger sequencing and checked for segregation within the available families. By analysis of the cDNA of P2 and P4, we verified that the consequences of some of these mutations on the mRNA level (the full pedigree charts and cDNA sequence are shown in Fig. 5). The mutation types included 4 frameshift (NM_001256714.1: c.679delC, p.(Leu227Serfs*28); NM_001256714.1: c.442delC, p.Leu148Trpfs*13; NM_001256714.1: c.388_432+60del; NM_001256714.1: c.811_815dupGACGC, p.Ala273Thrfs*13), 1 nonsense (NM_001256714.1: c.1465 C>T, p.Gln489*), and 1 missense (NM_001256714.1: c.200 C>A, p.Ser67Tyr). Except for the frameshift mutations (c.811_815dupGACGC, p.Ala273Thrfs*13), which are present in ClinVar, the other mutations had not been previously reported and were not present in the current ClinVar, dbSNP, 1000 human genome dataset, nor ExAC nor found local normal controls. The majority of mutations are either frameshift or nonsense mutations, leading to a loss of function by causing truncation of the encoded proteins.

c.679delC could result in a reading frameshift during translation at leucine 227, followed by a premature stop codon at position 254, possibly leading to a truncated protein, and c.442delC causes a frameshift that may lead to generates 12 novel amino acids after a p.Leu148Trp change followed by a premature stop codon (p.Leu148Trpfs*13). The frameshift mutation (c.388_432+60del) spans the exon3 and intron3 regions of *DNAAF3*. The 105-bp deletion is predicted to cause a splicing aberration, such as exon skipping or intron insertion, which could damage protein coding. The previously reported mutation c.811_815dupGACGC causes a frameshift that may generate 12 novel amino acids after a p.Ala273Thr change followed by a premature stop codon (p.Ala273Thrfs*13), and c.1465 C>T, p.Gln489*, the nonsense mutation, could result in the early termination of protein translation. c.200 C>A, p.Ser67Tyr is a missense mutation that could affect an amino acid residue which is evolutionary conserved in *DNAAF3* orthologues (*Mus musculus, Takifugu rubripes, Danio rerio, Drosophila melanogaster*). Programs predicting

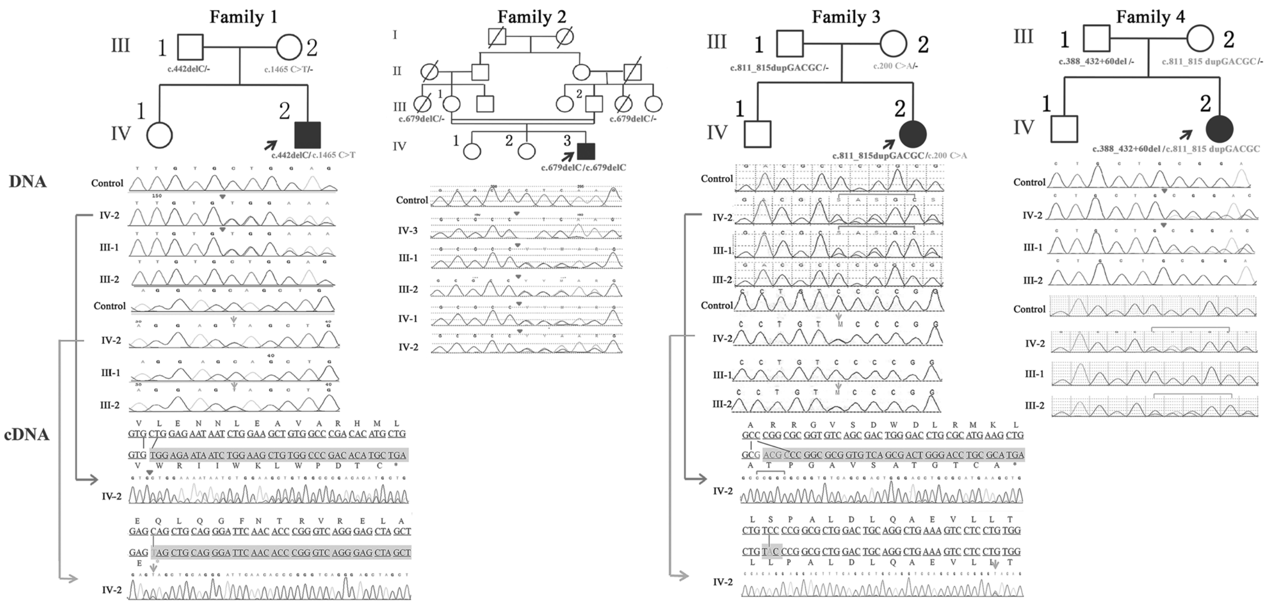


**Fig. 5** Pedigree of the families, and genomic DNA and cDNA sequencing chromatogram of the patients. Roman numerals refer to generations, and individuals within a generation are numbered from left to right. Black circles/squares are affected, and white circles/squares are unaffected. P1–P4 are the probands. The Sanger sequencing chromatogram of the patient, available family members, and a control are shown under each pedigree. ↓: single-base substitution mutation; ▼: deletion mutation; and ┌─┐: insertion mutation

functional consequences considered this amino acid exchange change to be pathogenic (MutationTaster: disease causing, Provean: deleterious, SIFT: damaging).

## Discussion

In the present study, WES was conducted and to identify the causative genes in four Chinese patients with PCD. A total of 7 variants in *DNAAF3*, which include 1 homozygous variant and 6 heterozygous variants, were identified and cosegregated in their families. The reported mutation c.811_815dupGACGC was identified both in P3 and P4, while the other 5 mutations (c.679delC, c.442delC, c.388_432+60del, c.1465 C>T, c.200 C>A) were novel to this study. As expected, the parents were heterozygous and the probands were homozygous or compound heterozygous in accordance with the autosomal-recessive mode of inheritance of PCD. To the best of our knowledge, the present study is the first to report *DNAAF3* mutations in PCD patients in China.

The contribution of *DNAAF3* to PCD was first realized in 2012 [9]. In affected members of 3 unrelated consanguineous families with PCD, Mitchison et al. identified 3 different homozygous mutations in *DNAAF3*. Then, they carried out functional analyses of *DNAAF3* in zebrafish and *Chlamydomonas* and found that *DNAAF3* plays an important role in a later step in the dynein assembly process, which plays a crucial role in cilium motility. Consistent with the findings of Mitchison et al., HSVA and a TEM examination showed that the respiratory cilia were completely paralyzed and characterized by ODA plus IDA defects in our research, providing strong evidence that *DNAAF3* is essential for the assembly of dynein arms and that these mutations are responsible for the patients' symptoms.

Measurement of the nNO level is a simple method that is recommended as part of the diagnostic work-up of PCD [10]. It is generally recognized that nNO is extremely low in PCD patients. Recently, however, a higher level of nNO in PCD patients with certain genotypes has been noticed, for unknown reasons [7, 18, 19]. As the first report of the nNO level in patients with *DNAAF3* mutations, our results show that the nNO level of these patients is only approximately a tenth of the normal value [12, 20].

Lung function and radiological examinations were performed to understand the effect of *DNAAF3* mutations in our patients. In the present research, situs inversus was present in all patients, consistent with dnaaf3 morphant zebrafish indicating that *DNAAF3* plays an important role in left–right determination during early embryogenesis. The respiratory symptoms of the patients in the present study appeared to be mild. The main respiratory symptom was intermittent coughing without obviously recurrent lower respiratory infections. Chest CT revealed that the lung lesions in these patients were subtle, consistent with their near normal lung function. Recently, two large-scale prospective studies [8, 21] have investigated the associations between ultrastructural defects with the clinical phenotype in pediatric populations. The data from a total of 255 PCD children underwent were systematically analyzed. It was found that patients with ODA plus IDA defects had a better percent predicted FEV1 than subjects with central apparatus defects with microtubular disorganization (91% vs 72% [8]; 85.5% vs 71.5% [21]). It is worth mentioning that there was only one patient with ODA plus IDA defects with *DNAAF3* mutations identified in the above-mentioned cohort (out of a total of 255 cases). In the Mitchison et al. report, all affected adults manifested with clinical features consistent with PCD, including recurrent upper and lower airway disease with chronic cough. Four of the ten affected adults were situs inversus totalis, five had otitis media, two had hearing impairment, and one suffered from neonatal respiratory distress syndrome. The patients who had a c.323 T>C mutation had severe respiratory symptoms, including chronic cough, hemoptysis, and bilateral bronchiectasis. To date, the reported sample size of patients with *DNAAF3* mutations is too small to make a definitive conclusion about the natural history of pulmonary involvement.

Rather than the typical PCD phenotype, certain PCD-pathologic genes have been reported to be associated with normal nNO level, ciliary ultrastructural appearance, and beat frequency, which complicates the diagnosis of PCD. Our data showed that patients with *DNAAF3* mutations have a typical PCD phenotype, including a low nNO level and completely paralyzed cilia, which makes it possible to identify patients with *DNAAF3* mutations by the routine diagnostic work-up for PCD.

There are some limitations in our study. First, cDNA sequencing was performed on only some of the patients due to the limitations of sampling, but it was valuable to exclude these mutations from activating cryptic splice sites. However, there is still a need for further research to better delineate the pathomechanisms of patients with *DNAAF3* mutations. Second, we found that the symptoms of the lower respiratory tract in patients with *DNAAF3* mutations were mild in childhood, which should be taken with care considering that the number of patients is small. A larger number of patients and greater length of follow-up are needed to better appreciate the clinical characteristics of patients with *DNAAF3* mutations.

In summary, as the first report on *DNAAF3* mutations in PCD patients in China, our study not only expands the spectrum of *DNAAF3* mutations but also further complements the detailed phenotype characteristics of these patients.

**Acknowledgements** This study was supported by the National Natural Science Foundation of China (81471481), the Development Fund for Shanghai Talents (201450), and the Open Research Project of the Shanghai Key Laboratory of Birth Defects (16DZKF1012).

**Author contributions** Zhuoyao Guo and Weicheng Chen performed the research, analyzed and interpreted the data, and drafted the manuscript. Jianfeng Huang designed the study and analyzed the data. Libo Wang and Liling Qian conceived and designed the study, revised the manuscript, and provided final approval of the manuscript.

## Compliance with ethical standards

**Conflict of interest** The authors declare that they have no conflict of interest.



## References

1. Reula A, Lucas JS, Morenogaldó A, Romero T, Milara X. New insights in primary ciliary dyskinesia. Expert Opin Orphan Drugs. 2017;5:537–48.
2. Knowles MR, Daniels LA, Davis SD, Zariwala MA, Leigh MW. Primary ciliary dyskinesia. Recent advances in diagnostics, genetics, and characterization of clinical disease. Am J Respir Crit Care Med. 2013;188:913–22.
3. Fliegauf M, Benzing T, Omran H. When cilia go bad: cilia defects and ciliopathies. Nat Rev Mol Cell Biol. 2007;8:880–93.
4. Bonnefoy S, Watson CM, Kernohan KD, Lemos M, Hutchinson S, Poulter JA, et al. Biallelic mutations in LRRC56, encoding a protein associated with intraflagellar transport, cause mucociliary clearance and laterality defects. Am J Hum Genet. 2018;103:727–39.
5. Loges NT, Antony D, Maver A, Deardorff MA, Güleç EY, Gezdirici A, et al. Recessive DNAH9 loss-of-function mutations cause laterality defects and subtle respiratory ciliary-beating defects. Am J Hum Genet. 2018;103:995–1008.
6. Fassad MR, Shoemark A, Borgne PI, Koll F, Patel M, et al. C11orf70 mutations disrupting the intraflagellar transport-dependent assembly of multiple axonemal dyneins cause primary ciliary dyskinesia. Am J Hum Genet. 2018;5:956–72.
7. Knowles MR, Ostrowski LE, Leigh MW, Sears PR, Davis SD, Wolf WE, et al. Mutations in RSPH1 cause primary ciliary dyskinesia with a unique clinical and ciliary phenotype. Am J Respir Crit Care Med. 2014;189:707–17.
8. Davis SD, Ferkol TW, Rosenfeld M, Lee HS, Dell SD, Sagel SD et al. Clinical features of childhood primary ciliary dyskinesia by genotype and ultrastructural phenotype. Am J Respir Crit Care Med. 2015;191:316–24.
9. Mitchison HM, Schmidts M, Loges NT, Freshour J, et al. Mutations in axonemal dynein assembly factor DNAAF3 cause primary ciliary dyskinesia. Nat Genet. 2012;44:381–9.
10. Lucas JS, Barbato A, Collins SA, Goutaki M, Behan L, Caudri D, et al. European Respiratory Society guidelines for the diagnosis of primary ciliary dyskinesia. Eur Respir J. 2017;49:1601090.
11. American Thoracic Society, European Respiratory Society. ATS/ERS recommendations for standardized procedures for the online and offline measurement of exhaled lower respiratory nitric oxide and nasal nitric oxide. Am J Respir Crit Care Med. 2005;171:912–30.
12. Beydon N, Chambellan A, Alberti C, de Blic J, Clement A, Escudier E, et al. Technical and practical issues for tidal breathing measurements of nasal nitric oxide in children. Pediatr Pulmonol. 2015;50:1374–82.
13. DePristo MA, Banks E, Poplin R, Garimella KV, Maguire JR, Hartl C, et al. A framework for variation discovery and genotyping using next-generation DNA sequencing data. Nat Genet. 2011;43:491–8.

14. Yang L, Kong Y, Dong X, Hu L, Lin Y, Chen X, et al. Clinical and genetic spectrum of a large cohort of children with epilepsy in China. Genet Med. 2018. https://www.ncbi.nlm.nih.gov/.
15. Richards S, Aziz N, Bale S, Bick D, Das S, Gastier-Foster J, et al. Standards and guidelines for the interpretation of sequence variants: a joint consensus recommendation of the American College of Medical Genetics and Genomics and the Association for Molecular Pathology. Genet Med. 2015; 17:405–24.
16. Fromer M, Pocklington AJ, Kavanagh DH, Williams HJ, Dwyer S, Gormley P, et al. De novo mutations in schizophrenia implicate synaptic networks. Nature. 2014;506:179–84.
17. Leigh MW, Hazucha MJ, Chawla KK, Baker BR, Shapiro AJ, Brown DE, et al. Standardizing nasal nitric oxide measurement as a test for primary ciliary dyskinesia. Ann Am Thorac Soc. 2013;10:574–81.
18. Olbrich H, Cremers C, Loges NT, Werner C, Nielsen KG, Marthin JK, et al. Loss-of-function GAS8 mutations cause primary ciliary dyskinesia and disrupt the nexin–dynein regulatory complex. Am J Hum Genet. 2015;97:546–54.
19. Shoemark A, Moya E, Hirst RA, Patel MP, Robson EA, Hayward J, et al. High prevalence of *CCDC103* p.His154Pro mutation causing primary ciliary dyskinesia disrupts protein oligomerisation and is associated with normal diagnostic investigations. Thorax. 2018;73:157–66.
20. You S, Zhang J, Bai Y, Ji L, Wang H. Normal values of nasal NO and exhaled NO in young Chinese people aged 9–22 years. World J Otorhinolaryngol Head Neck Surg. 2016;2:22–7.
21. Davis SD, Rosenfeld M, Lee HS, Ferkol TW, Sage SD, et al. Primary ciliary dyskinesia: longitudinal study of lung disease by ultrastructure defect and genotype. Am J Respir Crit Care Med. 2019;199:190–8.